Materials Research. 2018; 21(1): e20170041
DOI: http://dx.doi.org/10.1590/1980-5373-MR-2017-0041

MgO Saturation Analisys of $CaO-SiO_2-FeO-MgO-Al_2O_3$ Slag System

Rodolfo Arnaldo Montecinos de Almeida[a]*, Deisi Vieira[a], Wagner Viana Bielefeldt[b], Antônio Cezar Faria Vilela[b]

[a]Laboratório de Siderurgia - LaSid, Universidade Federal do Rio Grande do Sul - UFRGS, Porto Alegre, Rio Grande do Sul, Brazil
[b]Laboratório de Siderurgia - LaSid, Departamento de Metalurgia, Universidade Federal do Rio Grande do Sul - UFRGS, Porto Alegre, Rio Grande do Sul, Brazil

Received: January 16, 2017; Revised: August 04, 2017; Accepted: August 18, 2017

Electric arc furnace (EAF) slag has a range of functions, including improving energy efficiency through the "slag foaming" phenomenon. As such, the study of slag is important in EAFs. One of the factors that determine foaming quality and efficiency is the presence of solid particles. MgO saturation is highly significant since, in addition to ensuring the presence of solid particles, it also ensures chemical compatibility to minimize refractory consumption. The present study aims to examine MgO saturation, using the software FactSage v.6.4 for all calculations, in the $CaO-SiO_2-FeO-MgO-Al_2O_3$ slag system and the influence of binary basicity, FeO and Al_2O_3 content on this system. Ternary diagrams revealed the influence of Al_2O_3 content on the liquid field and other phases present. Isothermal saturation diagrams (ISDs) were constructed, showing the same dual saturation points found in the ternary diagrams. The ISDs were validated by comparing the results of different heats in terms of the electrical energy consumption. The closer the heat is to the MgO saturation line, the less energy is consumed.

Keywords: *EAF, MgO saturation, Dual saturation.*

1. Introduction

Slag plays different roles in electric arc furnaces, from protecting refractories against arc radiation to absorbing phosphorus and improving energy efficiency.

However, in order to satisfactorily perform these roles, slag composition must be compatible with the refractories used in the furnace. They are typically made of basic oxides (MgO, CaO, etc.) and end up being incorporated to the slag throughout the EAF process, as primary refining slag is rich in acidic oxides (SiO_2, MnO, FeO, etc.). Thus, it must have the correct basicity and be MgO saturated.

Table 1 shows an example of EAF primary refining slag.

Excess MgO and proper basicity minimize refractory consumption and contribute to the foaming phenomenon. For foaming to occur, slag must contain excess oxygen and carbon, according to the following reactions 1 and 2.

$$\underline{C} + \frac{1}{2}O_2 \rightarrow CO \qquad \text{(Reaction 1)}$$

$$C + (FeO) \rightarrow CO + \underline{Fe} \qquad \text{(Reaction 2)}$$

As CO bubbles are generated by these reactions, slag expands and covers the arc. There are several parameters that a good foaming slag: adequate viscosity, low surface tension, low density[2], and the presence of solid particles[3]. Slag saturation in CaO and MgO produces solid particles that serve as bubble nucleation sites, generating a larger amount of small bubbles[3].

Studying slag foaming is highly complex and involves variables such as temperature, basicity, the chemical composition of slag, and MgO saturation. Thus, the present study aimed to analyze MgO saturation behavior in the $CaO-SiO_2-MgO-FeO-Al_2O_3$ system according to different slag chemical composition parameters, at a temperature of 1600°C, using FactSage 6.4 thermodynamic simulation software.

2. Materials and Methods

FactSage was created in 2001, resulting from the merge of two well-known software packages in the field of computational thermochemistry: FACT-Win (formely F*A*C*T) and ChemSage (formerly SOLGASMIX). According to Bale *et al.*[4-6], this software is under constant development, whether upgrading or adding new database.

Several studies have been carried out to validate the database, from binary[7,8], quaternaries[9-11], and even more complex systems[12-14]. In these studies the "quasichemical" model[15] was used for the themodynamic description and, among them, some were performed to evaluate systems containing iron oxide (both FeO and Fe_2O_3)[9,11,13,14].

The software FactSage 6.4 was used for all calculations in this study. This software has been used in several studies of primary[16,17] and secondary[18,19] refining slag.

*e-mail: rodolfo.almeida@ufrgs.br

Table 1. Main EAF slag components and final composition %[1].

Component	Component range
CaO	25 - 40
SiO_2	5 - 20
MgO	7 - 13
FeO	20 - 45
Al_2O_3	2 - 10
MnO	2 - 5
P_2O_5	< 1,5

The following databases were used:

- FToxid: this database consists of two sections: FToxid53Soln.sda, which contains evaluated/optimized oxide solutions, and FToxid53Base.cdb, for evaluated and optimized solid and liquid compounds. The main oxides in this database are: Al_2O_3, CaO, FeO, Fe_2O_3, MgO, SiO_2[20].
- FactPS: pure substance database.

In iron and steel production slags, not all iron oxide present is in the form of FeO. In fact, Fe_2O_3 also exists. The higher valence iron oxide (Fe^{3+}), probably located in the slag region in contact with air, will be unstable in the slag region that is in physical contact with liquid iron[21]. This study adopted the system CaO-SiO_2-MgO-Al_2O_3-FeO, using FeO instead of Fe_2O_3.

It is known that the Fe^{3+}/Fe^{2+} relation decreases when the silica content is increased[22], increases with increasing slag basicity[22,23] and with decreasing Fe_tO content in basic slags[22]. Tayeb *et al.*[24] performed calculations of the Fe^{3+}/Fe^{2+} ratio in FactSage software, comparing to experimental results published by other authors. For an iron oxide ranging from 10 to 20 wt pct, FactSage predict a Fe^{3+}/Fe^{2+} ratio of 0.12 to 0.18[24], which is in good agreement with the literature[22].

Because the Fe_2O_3 phase is acidic in a basic slag, the MgO solubility could be increased. However Tayeb *et al.*[24] calculated the change in solubility of MgO by replacing FeO by Fe_2O_3 in FactSage, resulting in a small increase on MgO solubility (<1 wt. pct). Thus, considering that all the iron oxides are in the form of FeO will not lead to errors in the MgO saturation calculated by FactSage.

The effect of binary basicity on MgO saturation was analyzed for FeO contents between 15 and 35 weight %. The calculations were done for different basicities (1.5, 2.0, 2.5 and 3.0). In this analysis the chemical compositions were pre-established by the authors. As FeO increases in the analysis, the CaO and SiO_2 decrease, but the basicity relation (B_2=%CaO/%SiO_2) is constant.

To study the behavior of the MgO saturation due to temperature change, data were pre-stablished, the FeO content for all the analysis was constant (30% wt.) and the basicity varied between 1.5 and 3.0. The calculations were done for different temperatures (1500, 1550, 1600 and 1650 °C).

In order to make comparisons and determine the effect of Al_2O_3 on the CaO-SiO_2-FeO-MgO system, CaO-SiO_2-FeO pseudo-ternary diagrams with 5% MgO and different Al_2O_3 values (0, 5 and 8%) were made using FactSage software v. 6.4.

Isothermal Saturation Diagrams (ISDs), introduced by Pretorius[3] can also be used to analyze MgO saturation. ISDs are compiled considering two main boundary conditions: constant basicity and constant temperature. Figure 1 shows a generic ISD.

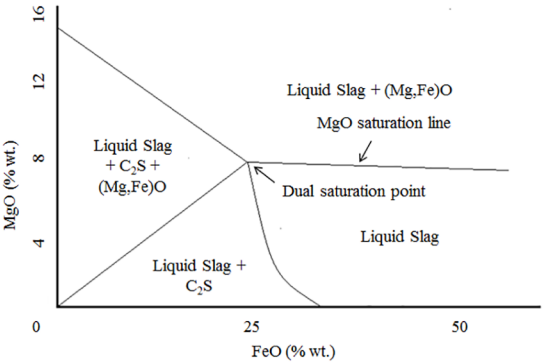

Figure 1. Generic isothermal saturation diagram.

Figure 1 shows some of the main information provided by ISDs: FeO and MgO content necessary for dual saturation to occur; the point C (whose chemical composition can be obtained from the chemical composition of the liquid in the FeO-MgO diagram); and the line connecting the dual saturation point and point C, named MgO saturation line[25].

It is known that ISDs reflect MgO saturation and that slag foaming is favored by the presence of solid particles. Therefore, when the MgO content in the heat is slightly above the saturation line but close enough to it, it is going to provide higher quality foaming and increase energy efficiency.

In order to evaluate the ISDs, historic data provided by a special steel mill was used. This data corresponded to heats produced using very similar scrap loads, regarding amount and scrap grades. Additionally, heats with the same chemical composition (basicity and Al_2O_3 content), similar refining times, and tapping temperatures varying by a maximum of 10°C were compared, based on their position in the ISD and their energy consumption.

3. Results and Discussion

3.1 Effects of binary basicity and FeO content

It is known that higher binary basicity slags, require lower MgO content for saturation[16] and that the FeO content significantly influences MgO saturation[26]. This can be seen in figure 2, which shows MgO saturation levels for different FeO contents for binary basicities ranging from 1.5 to 3.0.

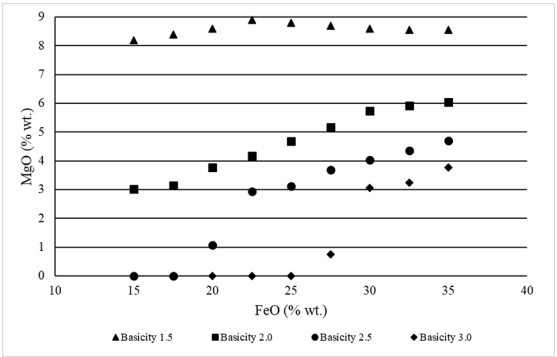

Figure 2. Effect of basicity on MgO saturation levels for different FeO contents at 1600°C.

Figure 2 shows that different behaviors occur at different basicities. For lower basicities, such as 1.5, MgO saturation varied slightly as FeO content changed. A different behavior is observed for basicities above 2.0 and 2.5; MgO saturation increases with increasing FeO contents. When basicity is increased even further, slag is MgO saturated until FeO content reaches approximately 25%. For higher FeOs, MgO is no longer saturated and behaves as it did in the previous cases. These last three cases show the fluxing effect FeO has on primary refining slag. Additionally, for the same FeO content, MgO saturation declines as basicity increases.

3.2 Effect of temperature

As the temperature rises, the liquid slag fraction increases and viscosity declines. That requires the MgO necessary for saturation to increase as well[16]. Figure 3 shows the behavior of MgO saturation with binary basicity at temperatures of 1500, 1550, 1600, and 1650 °C and 30% FeO.

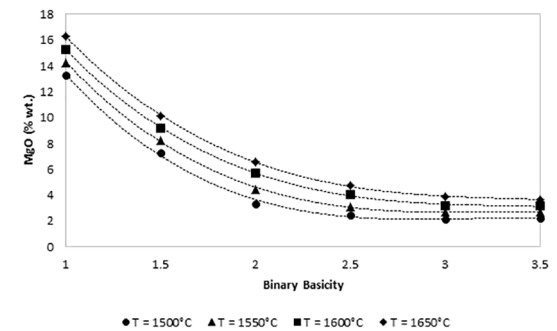

Figure 3. Chart showing MgO saturation content with binary basicity at temperatures of 1500 °C, 1550 °C, 1600 °C, and 1650 °C, and 30% FeO.

Figure 3 shows that, as basicity increases, MgO contents behave the same at all temperatures. Initially, there is a sharp decline (approximately 10%) between basicities from 1 to 2. At higher basicities, MgO can be considered constant.

Regarding temperature, MgO varies more with temperature at lower basicities, from 16.3% MgO at 1650°C to 13.3% MgO at 1500°C. The variation was smaller at a basicity of 3.5, from 3.6% MgO at 1650°C to 2.2% MgO at 1500°C.

3.3 Effect of Al_2O_3 content

3.3.1 Ternary diagrams

Another parameter that affects MgO saturation is Al_2O_3 content. In his study, Pretorius[3] used B_3 = %CaO/(%SiO_2+%Al_2O_3) to analyze this parameter, substituting a certain amount of silica with alumina to keep basicity constant. Pretorius[3] compared an alumina-free slag, resulting in binary basicity, with slag containing alumina, producing ternary basicity. To study the effect of Al_2O_3, the present study constructed CaO-SiO_2-FeO pseudo-ternary diagrams with fixed Al_2O_3 and MgO contents for comparison purposes. Figures 4 and 5 show the pseudo-ternary diagrams at 5% MgO, with and without Al_2O_3.

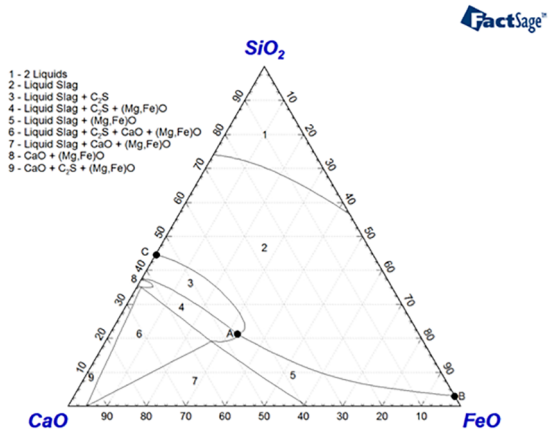

Figure 4. CaO-SiO_2-FeO pseudo-ternary diagram at 5% MgO and T = 1600°C.

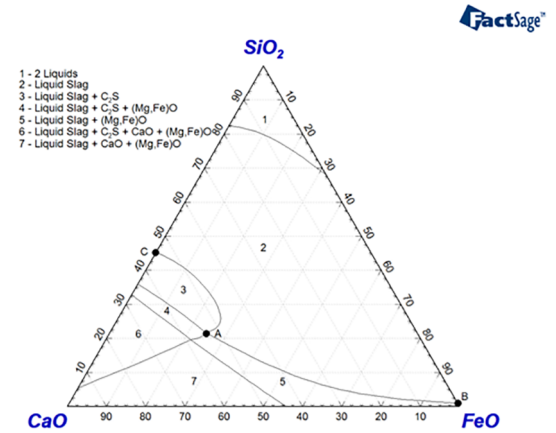

Figure 5. CaO-SiO_2-FeO pseudo-ternary diagram at 5% Al_2O_3 and 5% MgO, T = 1600°C.

The fields of particular interest for this study are 2, 3, and 5, consisting of: liquid, liquid + C_2S and liquid + (Mg, Fe) O, respectively. In other words, in field 3 CaO precipitates as C_2S ($2CaO.SiO_2$), and in field 5, MgO saturates as (Mg, Fe)O (magnesium wüstite). As such, A-C and A-B are C_2S and MgO saturation lines, respectively. At 5% Al_2O_3 (figure 5), the field consisting of C_2S + magnesium wüstite (field 8 in figure 4) is suppressed, as is the field comprising solid CaO + C_2S + magnesium wüstite (field 9 in figure 4).

Figure 6 shows the overlapping of the liquid fields from the two ternary diagrams and the addition of liquid field lines for an Al_2O_3 content of 8%.

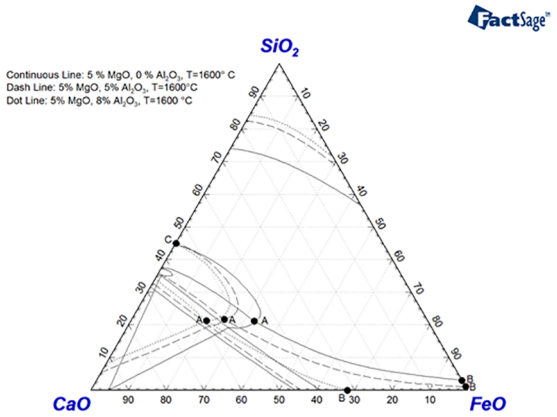

Figure 6. Superimposed liquid fields of the pseudo-ternary diagrams at 0%, 5%, and 8% Al_2O_3 and 5% MgO.

Figure 6 shows the differences in the liquid slag field (field 2) caused by Al_2O_3. The presence of Al_2O_3 causes the expansion of the liquid slag field, evident in the change in lines A-C and A-B.

Another important difference occurs for point A, which, according to Paulino[27], is the dual saturation point. In other words, this is the point where fields 2, 3, and 5 in figures 4 and 5 intersect, and where saturation occurs for both CaO as C_2S and MgO in the form of magnesium wüstite.

There was a significant change to point A with the change in Al_2O_3 content, as shown in table 2.

Al_2O_3 content significantly influences point A. Table 2 shows that the higher the Al_2O_3 content, the greater the basicity (from 2.15 at 0% to 2.78 at 8% Al_2O_3) and lower the FeO content needed for dual saturation. This indicates the flux effect of alumina, as demonstrated by Kim et al.[26].

3.3.2 Isothermal Saturation Diagrams

Given that ISDs are constructed using constant basicity and temperature, ISDs were compiled using the chemical compositions at point A in figure 6. The same basicities found and the same Al_2O_3 content were used, at the temperature of 1600°C. The FeO and MgO contents obtained in the pseudo-ternary diagrams for the dual saturation point (point A) were compared to the values found in the ISDs of figures 7, 8, and 9.

Table 2. Chemical composition of dual saturation points (point A) for slag at: a) 0% Al_2O_3, b) 5% Al_2O_3, and c) 8% Al_2O_3.

	a	b	c
SiO_2	20.21	19.40	18.35
CaO	43.60	48.46	51.12
B_2	2.15	2.50	2.78
FeO	30.59	22.13	17.50
Al_2O_3	0	5.0	8.0
MgO	5.0	5.0	5.0

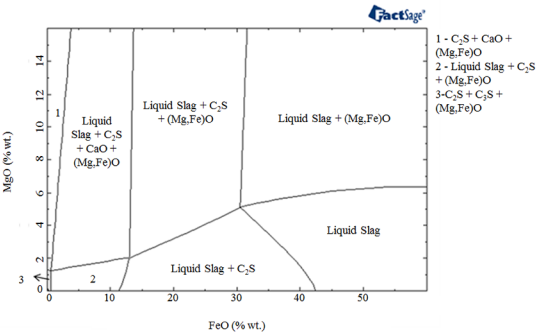

Figure 7. Isothermal Saturation Diagram B_2=2.15 and T = 1600°C.

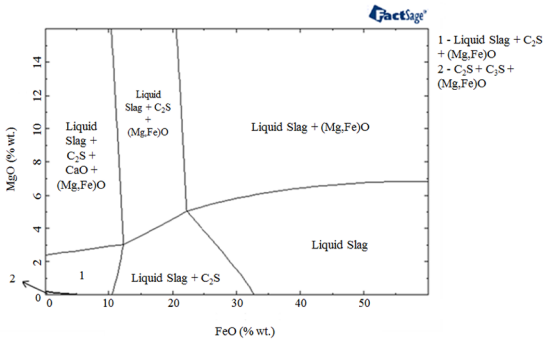

Figure 8. Isothermal Saturation Diagram B_2=2.5, 5% Al_2O_3, T=1600°C.

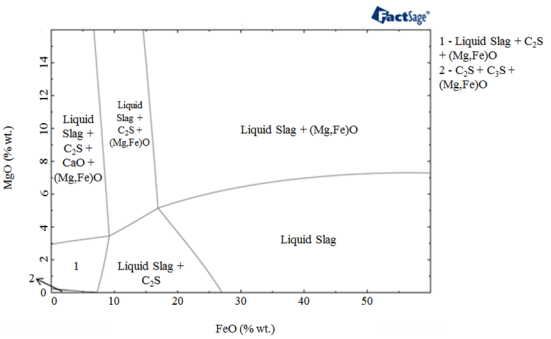

Figure 9. Isothermal Saturation Diagram B_2=2.78, 8% Al_2O_3, T=1600°C.

The ISD in Figure 7 was compiled for basicity of 2.15 and without the presence of Al_2O_3. The dual saturation point in this graph had the following chemical composition: FeO

content = 30.5 % and MgO content = 5.07 %. The ISD in figure 8 was constructed with basicity equal to 2.5; the dual saturation point was identified at FeO = 22.25% and MgO = 5.01%. In the ISD in figure 9, the dual saturation point found was: FeO = 16.95% and MgO = 5.14. When comparing these values to those shown in table 2, it is seen that the values are the same. That shows the ISDs can be used to predict the behavior of slag containing complex chemical composition that include Al_2O_3, for example.

The present study used ISDs to evaluate the effect of Al_2O_3 on MgO saturation. Differences are shown in figure 10. The graphs were superimposed in order to more easily visualize the binary basicities of 1.5, 2.0, 2.5, and 3.

Alumina has the same effect for all four basicities. Higher Al_2O_3 content leads to an increase in the MgO necessary for saturation and a decline in the FeO required for dual saturation, as observed in the ISD for basicity of 2.0, where the FeO necessary for dual saturation dropped from 30% (without Al_2O_3) to 15% (at 8% Al_2O_3). These two effects combined produce the same results seen in the pseudo-ternary diagrams, that is, the liquid field expands.

3.3.3 Tests using industrial data

It is known that solid particles serve as bubble nucleation sites, generating a larger amount of small bubbles[3], so slags saturated either in CaO or MgO should have a better foaminess than slags without solid particles or slags that are oversaturated in solid particles, resulting in less electric energy consumed.

Tests based on industrial data were conducted using electrical energy consumption during refining ($E_{refining}$) and the refining time ($T_{refining}$). The electrical energy consumption during refining ($E_{refining}$) is considered to be energy used after a flat bath state is reached inside the furnace (around 70% of the total electrical energy used in the heat). The heats plotted in the ISDs in figures 11, 12, and 13 had the same alumina content and basicity that were used to construct these ISDs. They show, for each heat, the $E_{refining}$, $T_{refining}$ and also the average electrical power (E_{Power}). The electrical power is relevant as it influences the refining time.

Figures 11 to 13 show the same behavior for all heats. Heats closer to the saturation line showed better results in terms of electrical energy consumption during refining and

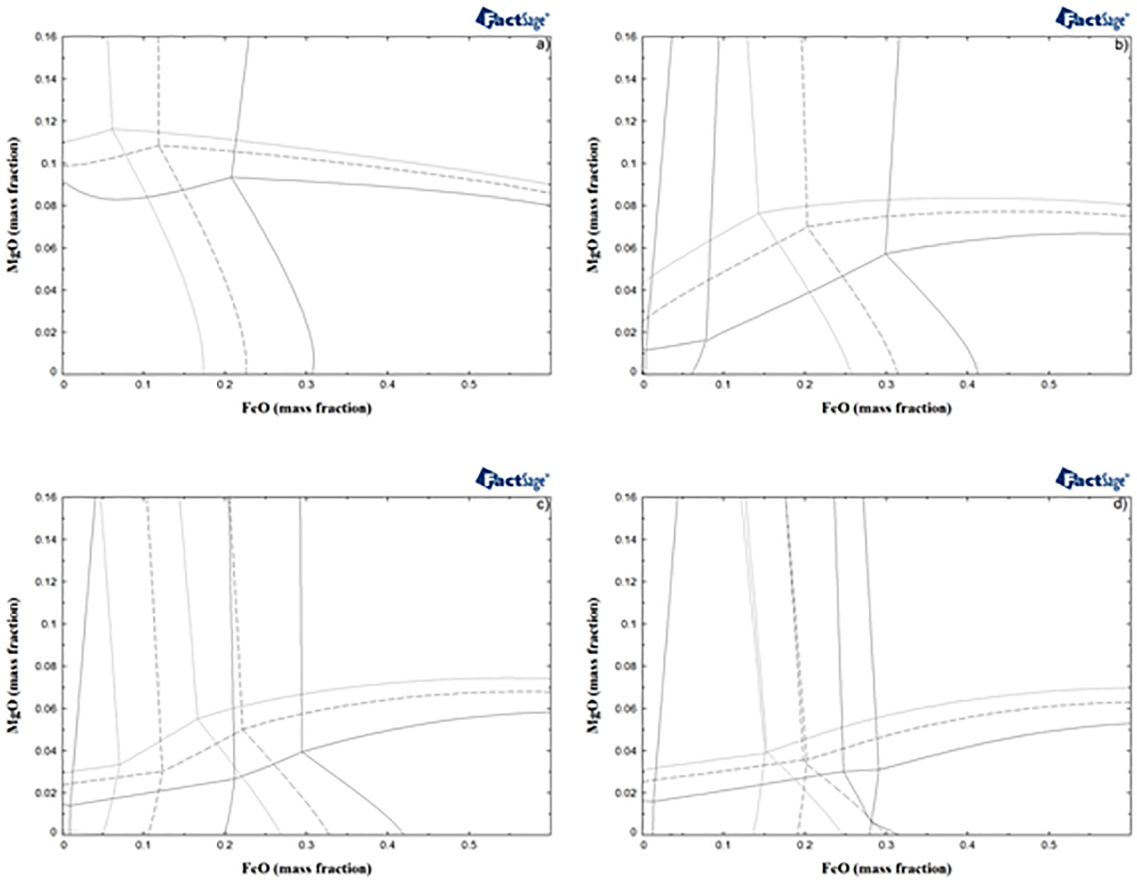

Figure 10. Isothermal saturation diagrams for different binary basicities, where continuous lines correspond to the absence of Al_2O_3, dashed lines the presence of 5% Al_2O_3, and dotted lines the presence of 8% Al_2O_3, T = 1600°C. (a) binary basicity 1.5; (b) binary basicity 2.0; (c) binary basicity 2.5; (d) binary basicity 3.0.

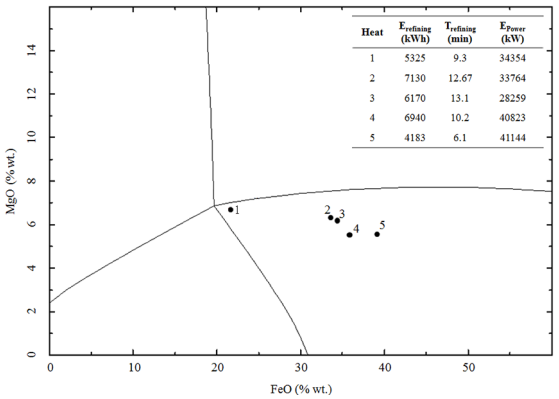

Figure 11. Isothermal saturation diagram 6.5% Al_2O_3, B_2=2.4, T=1600°C.

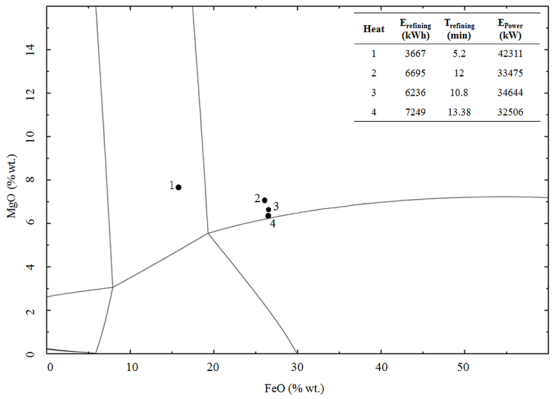

Figure 12. Isothermal saturation diagram 5.5% Al_2O_3, B_2=3.0, T=1600°C.

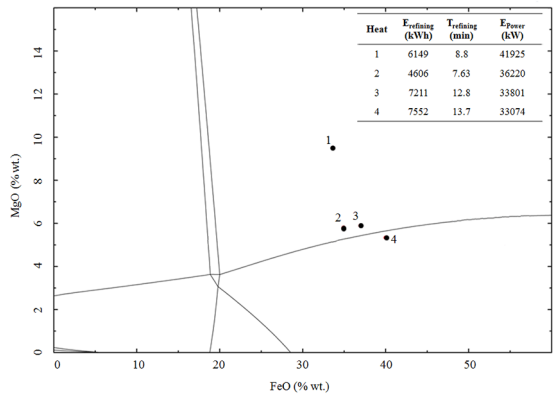

Figure 13. Isothermal saturation diagram 5.5% Al_2O_3, B_2=2.1, T=1600°C.

also refining time. The heats that are closer to the saturation line, showed similar electrical power (around 33000 kW) and the farther ones from the saturation line showed power above 40000 kW. In addition, heats with longer refining times resulted in higher energy consumption.

When heat 3 is analyzed (in figure 11), its electrical power is much lower than the others (28000 kW). This could mean that the heat might have had external factors that affected power (short electrode, for example). Excluding external factor, this heat could have had a higher power, using the same electrical energy but in shorter refining time.

Figure 12 shows the comparison between the three heats closer to the saturation line (heats 2, 3 and 4) and heat 1, farther from it. Despite the difference in refining times, there is a slight increase in energy consumption, and a significant decrease in power. For a refining time of 12.8 min (4 min difference), the energy increased by 1062 kWh. The energy increase was 1403 kWh when refining time was 13.7 min (5.9 min difference). A significant decrease in energy consumption (1543 kWh) was observed for the heat with a refining time of 7.6 min (1.2 min difference).

Except for 2 heats (heat 1 of figure 11 and heat 1 of figure 13) all other heats have similar FeO content, causing the variation of the electrical conductivity to be very low. Regarding the heats with different FeO, they had the same basicities as the other heats in their ISD. This indicates that these heats have higher CaO content. According to Jiao[28], the slag electrical conductivity can be expressed as an function of FeO, CaO e MgO. As all these oxides change (FeO decreases, and CaO and/or MgO increase), it can be considered that the electrical conductivity of these heats will be very similar. For this reason, electrical conductivity variations will not be taken into account.

4. Conclusions

- Results obtained using FactSage were in accordance with those expected for the relationship between basicity and MgO saturation, where the MgO necessary for saturation decreases as basicity increases. Regarding the relationship between FeO contents and MgO saturation: when basicities were 2.0 or higher, there was an increase in the MgO saturation. A different effect was observed for basicity of 1.5, with MgO saturation decreasing as FeO contents increased.
- The effect of Al_2O_3 was analyzed using CaO-SiO_2-FeO pseudo-ternary diagrams with 5% MgO and no Al_2O_3, as well as 5% and 8% Al_2O_3. Significant differences were observed in the liquid field and dual saturation points, with chemical composition changing from SiO_2 = 20.21%, CaO = 43.60% FeO = 30.59%, and MgO = 5% to SiO_2 = 19.40%, CaO = 48.46%, FeO = 22.13%, MgO = 5%, and Al_2O_3 = 5%, and SiO_2 = 18.35%, CaO = 51.12%, FeO = 17.50%, MgO = 5%, and Al_2O_3 = 8%, showing a major decrease in FeO content and an increase in basicity from 2.15 (without Al_2O_3) to 2.78 (8% Al_2O_3), for dual saturation to occur.
- The ISDs made for the points mentioned in the pseudo-ternary diagrams showed the same dual saturation points, with an MgO content of 5% and

FeO = 30.5% for a basicity of 2.15, MgO content = 5% and FeO = 22.25% for basicity 2.5, and FeO = 16.95% and MgO = 5.14 for basicity 2.78.

- The comparison of ISDs with and without alumina showed the flux effect of alumina, with a higher MgO content needed for saturation and lower FeO level required for dual saturation.
- ISDs can be used to analyze MgO saturation and energy consumption.
- Heats closer to the MgO saturation line resulted in lower power (around 33000 kW) than the farther ones (above 40000 kW).

5. Acknowledgements

Rodolfo Almeida would like to thank professors Wagner Bielefeldt and Antônio Vilela for their guidance and support, his LASID peers, and the CNPq for the research grant.

6. References

1. Turkdogan ET, Fruehan RJ. *The Making, Shaping and Treating of Steel, Vol. 2: Steelmaking and Refining*. Pittsburgh: The AISE Steel Fundation; 1998.

2. Morales RD, Rubén RG, López F, Camacho J, Romero JA. The Slag Foaming Practice in EAF and Its Influence on the Steelmaking Shop Productivity. *ISIJ International*. 1995;35(9):1054-1062.

3. Pretorius EB. Foamy Slag Fundamentals and their Practical Application to Electric Furnace Steelmaking. In: *Proceedings of the 55° ABM annual Congress*; 2000 Jul; Rio de Janeiro, RJ, Brazil.

4. Bale CW, Chartrand P, Degterov SA, Eriksson G, Hack K, Ben Mahfoud R, et al. FactSage thermochemical software and databases. *Calphad*. 2002;26(2):189-228.

5. Bale CW, Béslile E, Chartrand P, Decterov SA, Eriksson G, Hack K, et al. FactSage thermochemical software and databases - recent developments. *Calphad*. 2009;33(2):295-311.

6. Bale CW, Béslile E, Chartrand P, Decterov SA, Eriksson G, Gheribe AE, et al. FactSage thermochemical software and databases, 2010-2016. *Calphad*. 2016;54:35-53.

7. Wu P, Eriksson G, Pelton AD. Critical Evaluation and Optimization of the Thermodynamic Properties and Phase Diagrams of the CaO-FeO, CaO-MgO, CaO-MnO, FeO-MgO, FeO-MnO and MgO-MnO Systems. *Journal of the American Ceramic Society*. 1993;76(8):2065-2075.

8. Eriksson G, Pelton AD. Critical evaluation and optimization of the thermodynamic properties and phase diagrams of the CaO-Al_2O_3, Al_2O_3-SiO_2, and CaO-Al_2O_3-SiO_2 systems. *Metallurgical Transactions B*. 1993;24(5):807-816.

9. Decterov SA, Jung IH, Pelton AD. Thermodynamic Modeling of the FeO-Fe_2O_3-MgO-SiO_2 System. *Journal of the American Ceramic Society*. 2002;85(12):2903-2910.

10. Kang YB, Jung IH, Decterov SA, Pelton AD, Lee HG. Phase Equilibria and Thermodynamic Properties of the CaO-MnO-Al_2O_3-SiO_2 System by Critical Evaluation, Modeling and Experiment. *ISIJ International*. 2004;44(6):975-983.

11. Jung IH, Decterov SA, Pelton AD. Critical thermodynamic evaluation and optimization of the FeO-Fe_2O_3-MgO-SiO_2 system. *Metallurgical and Materials Transactions B*. 2004;35(5):877-889.

12. Decterov SA, Jung IH, Jak E, Kang YB, Hayes P, Pelton AD. Thermodynamic Modeling of the Al_2O_3-CaO-CoO-CrO-Cr_2O_3-FeO-Fe_2O_3-MgO-MnO-NiO_2-SiO_2-S System and Applications in Ferrous Process Metallurgy. In: *Proceedings of VII International Conference on Molten Slags, Fluxes and Salts*; 2004 Jan 25-28; Cape Town South Africa. Johannesburg; 2004. p. 839-849.

13. Jak E, Hayes P, Pelton A, Decterov S. Thermodynamic optimisation of the FeO-Fe_2O_3-SiO_2 (Fe-O-Si) system with FactSage. *International Journal of Materials Research*. 2007;98(9):847-854.

14. Hidayat T, Shishin D, Jak E, Decterov SA. Thermodynamic reevaluation of the Fe-O system. *Calphad*. 2015;48:131-144.

15. Pelton AD, Degterov SA, Eriksson G, Robelin C, Dessureault Y. The modified quasichemical model I-Binary solutions. *Metallurgical and Materials Transactions B*. 2000;31(4):651-659.

16. Bennet J, Kwong KS. Thermodynamic studies of MgO saturated EAF slag. *Ironmaking & Steelmaking*. 2010;37(7):529-535.

17. Luz AP, Ávila TA, Bonadia P, Pandolfelli VC. Thermodynamic simulation and isothermal solubility diagram as tools for slag foaming control. *Ceramics International*. 2011;37(7):2947-2950.

18. Bielefeldt WV, Vilela ACF, Heck NC. Evaluation of the Slag System CaO-MgO-Al_2O_3-SiO_2. In: *Proceedings of the 44th Steelmaking Seminar-International*; 2013 May 26-29; Araxá, MG, Brazil.

19. Bielefeldt WV, Vilela ACF, Heck NC. Thermodynamic Evaluation of the Slag System CaO-MgO-SiO_2-Al_2O_3. In: *Proceedings of the 68th ABM International annual Congress*; 2012 Jul 30 - Aug 2; Belo Horizonte, MG, Brazil.

20. Canada. Center for Research in Computational Thermochemistry. *FactSage Database Documentation*; 2015. Available from: <http://www.crct.polymtl.ca/fact/documentation/>. Access in: 03/03/2015.

21. Paulino MAS, Klug JL, Bielefeldt WV, Vilela ACF, Heck N. Obtenção de Escória Espumante em Forno Elétrico a Arco: Determinação das Composições para o Sistema CaO-SiO_2-MgO-FeO. In: *Proceedings of the 45th Steelmaking Seminar-International*; 2014 May 25-28; Porto Alegre, RS, Brazil.

22. Shim JD, Ban-Ya S. The solubility of Magnesia and Ferric-Ferrous Equilibrium in Liquid FeO-SiO_2-CaO-MgO Slags. *Transactions of The Iron and Steel Institute of Japan*. 1981;67:1735-1744.

23. Kimura H, Endo S, Yajima K, Tsukihashi F. Effect of Oxygen Partial Pressure on Liquidus for the CaO-SiO_2-FeO_x System at 1573. *ISIJ International*. 2004;44(12):2040-2045.

24. Tayeb MA, Assis AN, Sridhar S, Fruehan RJ. MgO Solubility in Steelmaking Slag. *Metallurgical and Materials Transactions B*. 2015;46(3):1112-1114.

25. Kwong KS, Bennet J. *Achieving MgO Saturated Foamy Slags in the EAF*. In: *Proceedings of the 59th Electric Furnace Conference*; 2001 Nov 11-14; Phoenix, AZ, USA.

26. Kim YJ, Min DJ. Effect of FeO and Al_2O_3 on the MgO Solubility in CaO-SiO_2-FeO-Al_2O_3-MgO Slag System at 1823 K. *Steel Research International*. 2012;83(9):852-860.

27. Paulino MAS, Klug JL, Bielefeldt WV, Vilela ACF, Heck NC. Estudo da Escória Espumante em Forno Elétrico a Arco. In: *Proceedings of the 69th ABM International Annual Congress*; 2014 Jul 21-25; São Paulo, SP, Brazil.

28. Jiao Q, Themelis NJ. Correlations of electrical conductivity to slag composition and temperature. *Metallurgical Transactions B*. 1988;19(1):133-140.